JOURNAL OF MATERIALS SCIENCE 7 (1972) 413-421

Evidence for the Control of the Critical Current Density of Nb-25% Zr Superconducting Wires by the Dislocation Substructure

I. MILNE
Central Electricity Research Laboratories, Kelvin Avenue, Leatherhead, Surrey, UK

Transmission electron microscopy of longitudinal sections of 250 μm diameter Nb-25% Zr wire has revealed that annealing treatments which maximise J_c can cause polygonisation of the as-drawn dislocation substructure, precipitation of α_{Zr}, precipitation of β_{Zr} or recrystallisation of β_{Nb}. It is argued that the polygonised structure is the one which is most effective in controlling J_c.

T_c data has provided some very useful information for assessing the constitutional state of the material.

1. Introduction

The current carrying capacity of a type II superconductor is controlled by its ability to prevent magnetic flux from moving. This flux can be pinned in position by metallurgical features such as a suitable dislocation substructure or a precipitate [1]. In Nb-Zr alloys, high critical current densities, J_c, have always been obtainable by simply cold working the material, [2] but invariably this property has been further improved by subsequent annealing [3-5].

The early work of Chandrasekhar *et al* [6] hinted that this increase was due to the superconducting properties of the "filamentary" dislocation structure which was produced on annealing. This proposition had little experimental basis and much of the later evidence tends to favour precipitation as the controlling influence. For low-field J_c enhancement in Nb-55% Zr, Shukovsky, Ralls, and Rose [7] observed that a fine dispersion of precipitate caused an increase in J_c while large scale precipitates caused a decrease. Low temperature annealing treatments were the most influential, indicating that α_{Zr} was a more important pinning centre than β_{Zr}. The influence of α_{Zr} was also stressed by Komata, Ishihara, and Tanaka [8] in studying J_c enhancement on annealing drawn wires of Nb-10% Zr and Nb-33% Zr. The greater influence of annealing occurred in the latter alloy, implying a volume fraction effect of the pinning centres. More recent evidence, however, [9] supports the role of β_{Zr} as the pinning constituent.

The Nb-Zr system is further confused by the extreme sensitivity of the phase diagram [10] to interstitial impurity levels [11-14]. An increase in the concentration of interstitial elements causes a lowering of the monotectoid temperature and an expansion of the β-decomposition loop. Hillmann and Pfeiffer [15] pointed out that most of the work done on this system has been performed on material annealed either in a poor vacuum or in a silica container; even in a good vacuum silica would be reduced by the zirconium resulting in oxygen contamination. This contamination can cause β_{Zr} to form prematurely in a GP zone type structure, which has a very strong influence on J_c.

It can be seen that there is much conflicting evidence about the flux-pinning constituents in Nb-Zr. Direct evidence from transmission electron microscopy has not yet been satisfactorily documented, although there are studies involving ribbon [16] or wire which had been flattened by rolling before thinning into electron transmission specimens [15], techniques which impose quite severe limitations on the interpretations obtained. This paper describes a study by electron transmission microscopy of specimens of Nb-25% Zr wire which had been previously used to investi-

gate the influence of annealing treatments on the superconducting properties of this material. Changes in transition temperatures and critical current densities are correlated with the microstructure in a way that leads to a better understanding of the most influential flux-pinning constituent in this alloy.

2. Experimental Procedure

The same samples which had been measured in the zero field critical current experiments of Milne and Ward [17] were used for all the studies described here. They were made from a composite wire with a 250 μm diameter Nb-25% Zr core and a Cu sheath metallurgically bonded to the core.

The Nb-Zr contained 85 ppm oxygen, 55 ppm nitrogen and less than 10 ppm hydrogen and because of the protection afforded by the copper sheath it is not thought that these quantities changed much during the vacuum annealing.

Transition temperatures were measured using an inductive apparatus built in this laboratory which is capable of an accuracy of $\pm$ 0.03 K. Specimens for transmission electron microscopy were prepared from longitudinal sections of the above samples by the following technique, which used the copper sheath to help develop a suitable profile. Faces were first ground on to the wire from opposite sides to make a thin ribbon in which the Nb-Zr was exposed on the ground faces only, being protected by the copper elsewhere. This ribbon was then electropolished, without agitation, in a solution of 85% H_2SO_4 (SG = 1.84):15% HF (40%) at room temperature and 20 V using a platinum wire cathode placed an inch or so from the specimen. Polishing was continued until holes appeared in the ribbon, a process which took some hours. Where the ground faces were initially parallel these holes appeared in the centre of the ribbon, in other cases they began at one edge of the Nb-Zr core and spread from there as polishing proceeded. In either case it was not necessary to mask the copper as it was almost passive under the polishing conditions, preventing edge attack on the Nb-Zr. This helped to develop a very even profile in the core material, and because of the extremely slow polishing action the thin areas did not disappear rapidly as the holes increased in size. Finally the copper was dissolved in 50% HNO_3, a treatment which did not impair the electropolished surface of the Nb-Zr alloy. Afterwards the specimens were cleaned by ultrasonic agitation in methanol before they were mounted for observation in the AEI EM 6 G electron microscope.

To minimise repetition and avoid confusion in sample labelling they will be referred to as in the following example: 500/1 means "annealed at 500°C for 1 h", 650/168 means "annealed at 650°C for 168 h (1 week)".

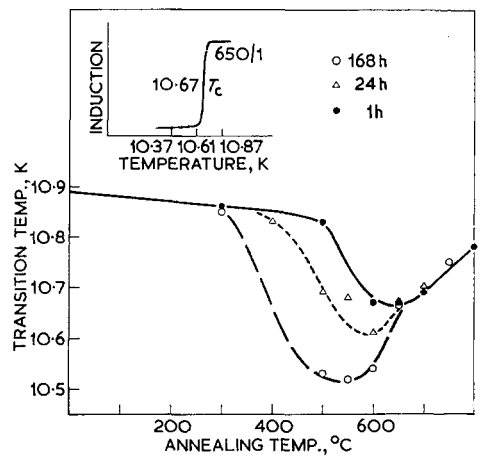

Figure 1 T_c versus annealing temperature. Isochronals for 168 h, 24 h and 1 h. The inset shows a typical transition and defines T_c.

3. Results

3.1. Transition Temperatures

The transition temperatures for 1 week, 24 h and 1 h anneals are shown in fig. 1. The inset depicts the transition curve of 650/1, a typical transition. The step is quite sharp and indicative of a fairly homogeneous material. The transition temperatures are defined as the temperature at half the step height of each transition curve. Each isochronal in fig. 1 shows the same characteristics; an initial stable region is followed by a minimum and then a rise. The minimum moved progressively to lower annealing temperatures as the annealing time was increased, the magnitude of the drop increasing. Above 650°C the curves coincide.

3.2. Electron Microscopy

3.2.1. 1 hour anneals

The electron micrographs reported in fig. 2 have been scaled to the same magnification (approximately × 100000) and are exhibited with their relevant selected area diffraction patterns. This sequence of micrographs scans the 1 h anneals from the as-drawn condition to 750°C, the

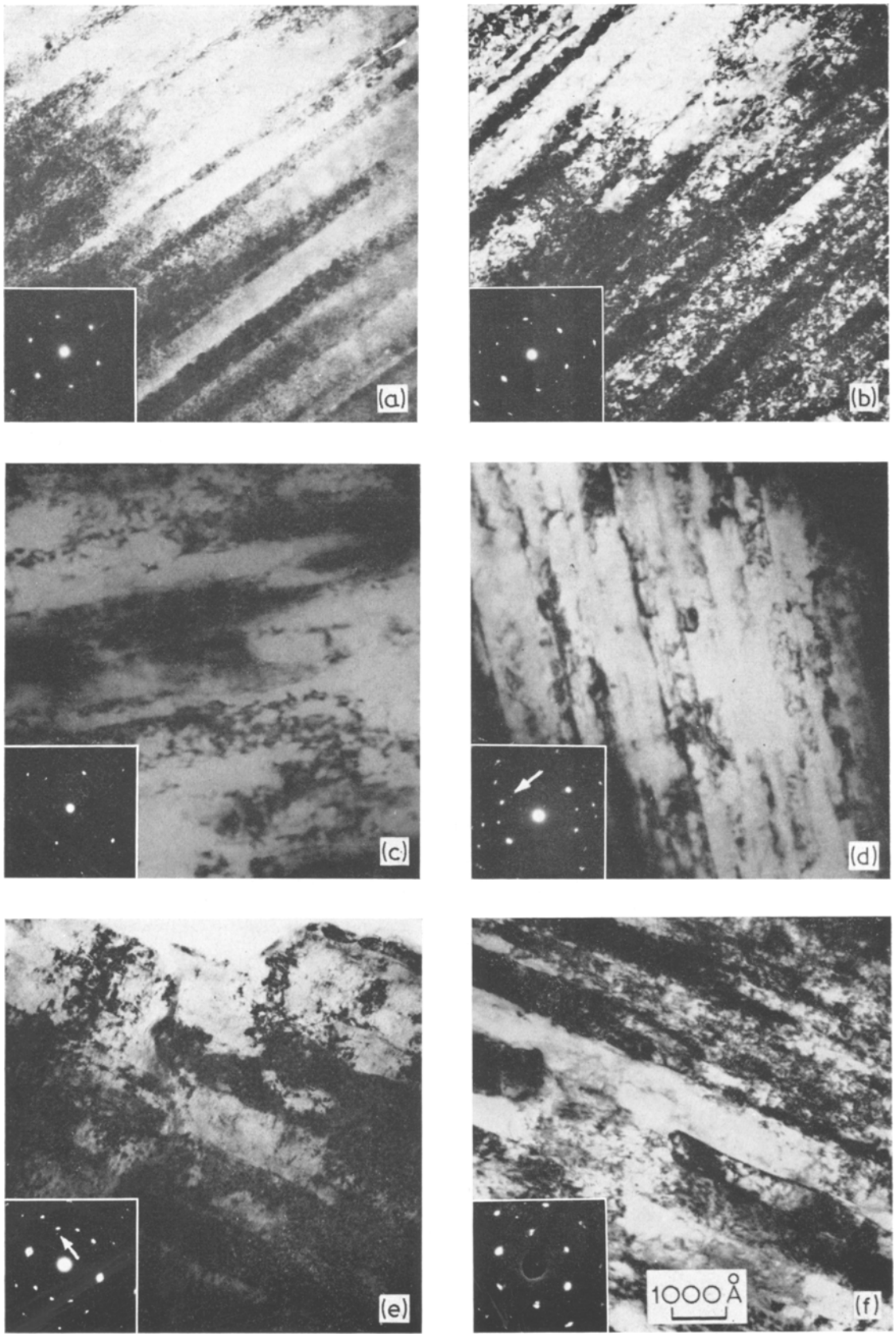

Figure 2 Electron transmission micrographs of specimens annealed for 1 h.

specimen exhibiting the highest J_c in the sequence. A $\langle 110 \rangle$ texture parallel to the drawing direction was maintained throughout. In most cases the diffraction patterns consisted of two overlapping patterns of $\langle 111 \rangle$ and $\langle 100 \rangle$ symmetry, and it was only occasionally that it was possible to obtain one of these without interference from the other. This was because of the rather fine fibrous structure which had developed and because the smallest diffraction aperture available in the electron microscope was 25 μm.

Indexing the diffraction spots of fig. 2a showed that some corresponded to $\langle 110 \rangle$ spots with a d-spacing equivalent to that of β_{Nb}, while others corresponded to a spacing between d-β_{Nb} and d-β_{Zr}. This is interpreted as relating to bcc Nb-25% Zr, the nominal composition of the material. This would be expected to be the main constituent in the as-drawn specimens, although small amounts of other phases would also be present, unavoidably formed when the material was worked at high temperatures during the manufacturing processes. These phases are responsible for the small amount of splitting in the matrix diffraction spots which could be observed from time to time in all specimens, as well as in the as-drawn. Occasionally the spots would be split into three and indexed as β_{Nb}, $\beta_{Nb\text{-}25\%Zr}$ and β_{Zr} respectively. A similar type of splitting was observed by Walker, Stickler, and Werner [16] on annealing Nb-25% Zr at low temperatures.

The as-drawn microstructure changed only slightly during annealing up to 500/1, but between this and 600/1, where the T_c approached its minimum, dislocation mobility became sufficient to cause more extensive recovery (fig. 2c). Here the dislocations which were previously scattered loosely in tangles have started to migrate into cell walls aligned linearly with the drawing direction. Some α_{Zr} was detected in the diffraction patterns, but could not be observed in the projected images. At 650/1 and 700/1 the second phase spots were more pronounced, as indicated by the arrows on the diffraction patterns of figs. 2d and e. They still indexed as α_{Zr}, however, contravening the phase diagram of Rogers and Atkins [10]. The dark field images reproduced in fig. 3 show the dispersion of the α_{Zr} responsible for these arrowed diffraction spots.

At 750/1, fig. 2f, the precipitate spots indexed as β_{Zr}, although it could not be revealed by dark field techniques.

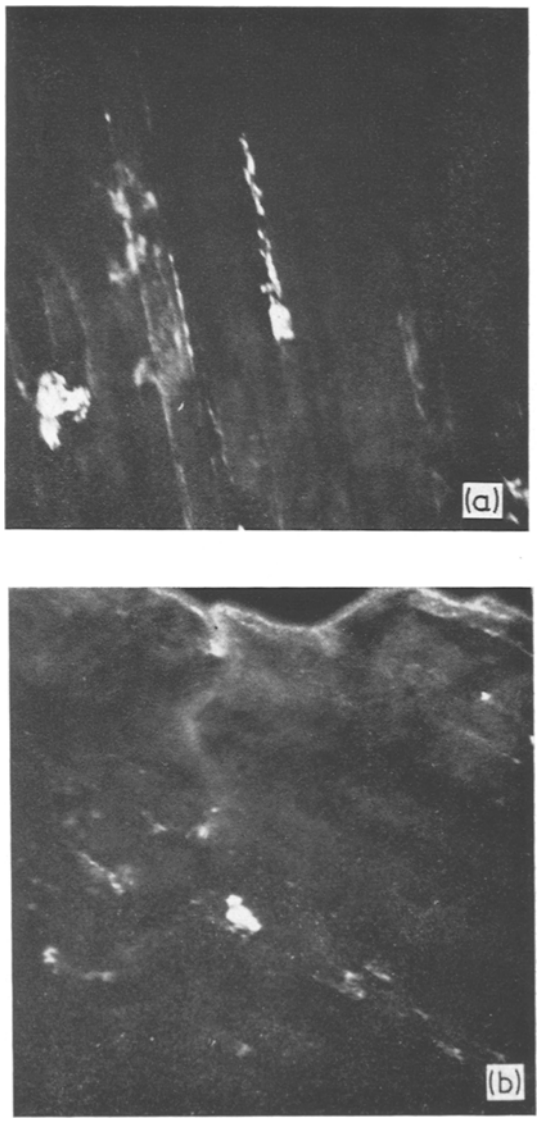

Figure 3 Dark field micrographs using α_{Zr} reflecting spots of (a) fig. 2d and (b) fig. 2e.

3.2.2. Peak J_c specimens

The highest J_c for 1 h anneals was obtained at 750/1 with the structure shown in fig. 2f. Equally high critical currents were obtained at 700/4, 650/24 and 550/168. The microstructures are reproduced in figs. 4a, b and c. The overaged structure of 750/2 is included in fig. 4d for comparison. All the high J_c microstructures showed the same well defined linear structure with sharp dislocation sub-boundaries. At the lower ageing temperatures when the optimum structure was only produced after long ageing times, regions of

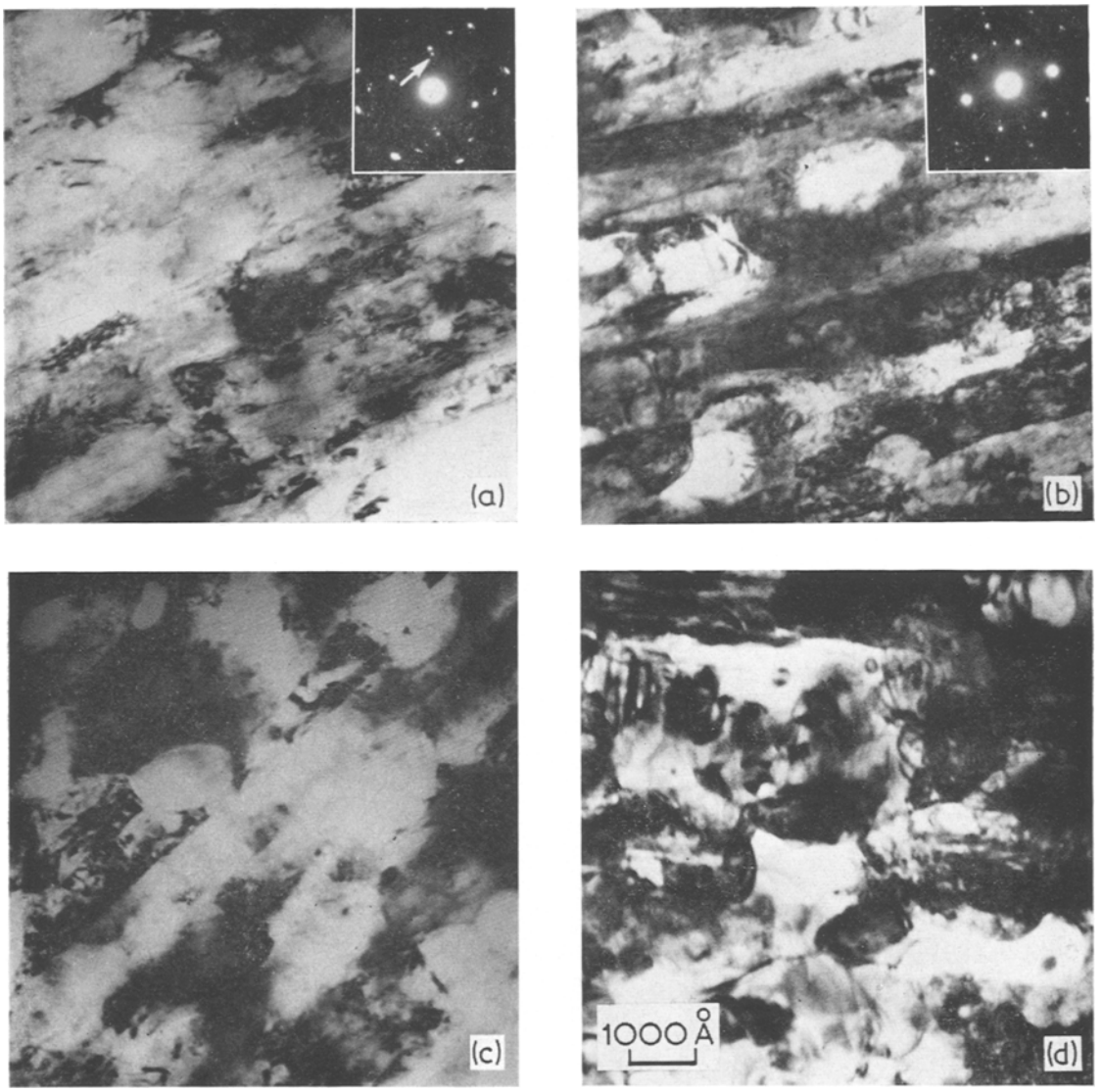

Figure 4 Electron transmission micrographs of specimens (a) 700/4, (b) 650/24, (c) 550/168 and (d) 750/2.

an equiaxed nature had also developed, particularly at 550/168 and 650/24. Selected area diffraction patterns over these regions indicated that α_{Zr} was again present (fig. 5a) but dark field microscopy (fig. 5b) showed that it was still forming as isolated precipitates. The dark field image (fig. 5d) of the arrowed β_{Nb} spot of fig. 5c shows that the equiaxed regions were β_{Nb}.

4. Discussion

Because of the confusion which surrounds the Nb-Zr phase diagram, it is not proposed to base the following argument too closely on it. Hillmann and Pfeiffer [15] confirmed that in pure specimens (< 100 ppm interstitials) the β decomposition loop did not appear, although it could be produced by annealing in air or introducing interstitials in some other way. The present specimens, containing some 140 ppm gaseous impurities, must therefore be considered to be on the borderline between pure and impure material. This suspicion is supported by the electron-diffraction data, which showed that β_{Zr} did not appear until the material had been annealed at 750°C or above, and this is in agree-

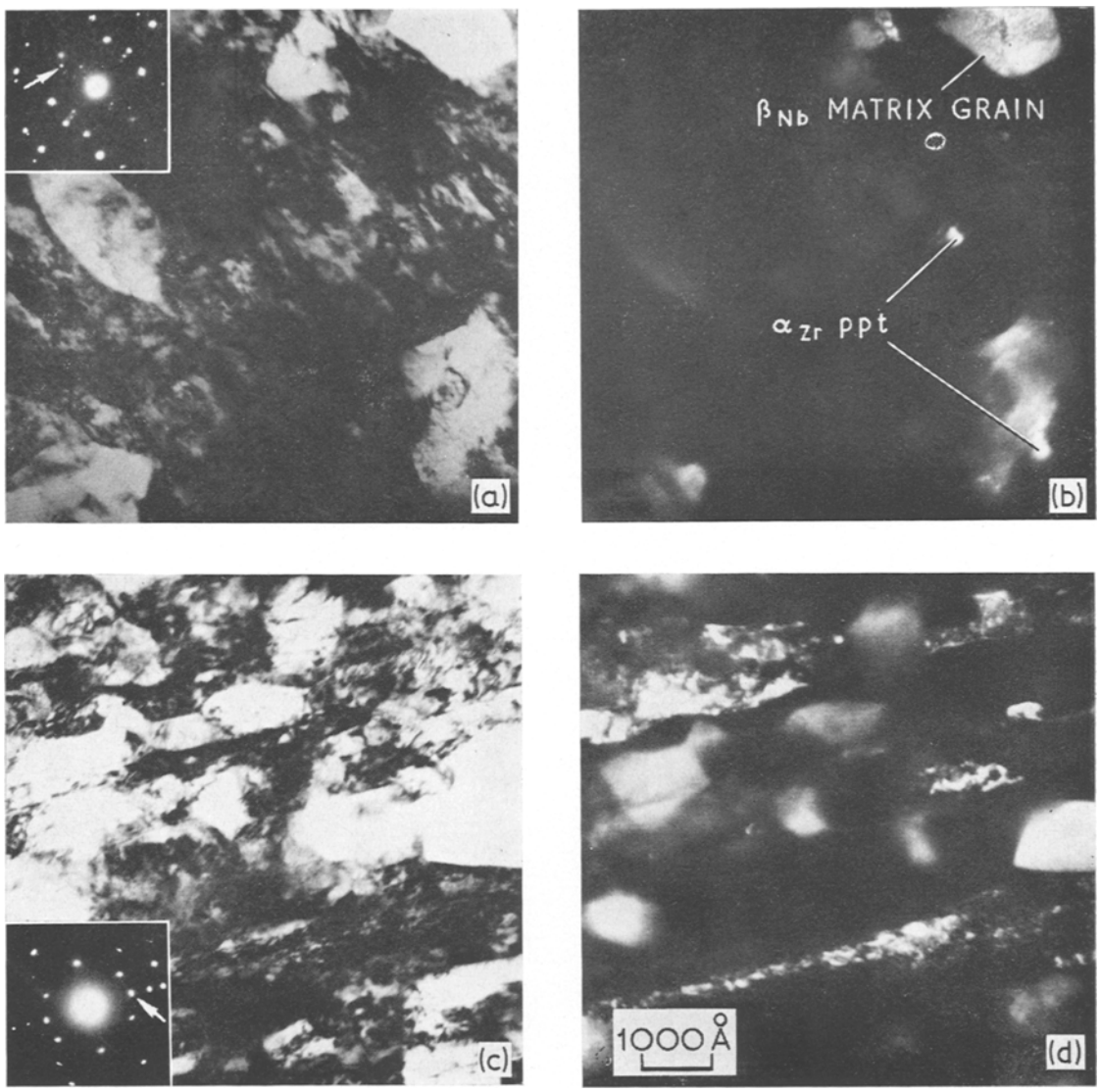

Figure 5 Electron transmission bright and dark field micrographs of 550/168 (a and b) 650/24 (c and d).

ment with the X-ray diffraction data cited by Milne and Ward [17].

4.1. Transition Temperatures

The transition temperature curves offer useful information about the annealing kinetics and the constitution of the specimens. Initially, all the specimens had the same T_c, that corresponding to a nominal composition of Nb-25% Zr. Departure from this occurred at progressively lower annealing temperatures, as the annealing time was increased, but the T_cs all returned to follow the same curve at 650°C, regardless of annealing time. Since T_c is primarily an intrinsic property of a superconductor [1] it is influenced mainly by the composition of the material. Therefore, between Nb and Nb-25% Zr, where T_c is known to increase monotonically [18, 19] it can be used to indicate the composition of the matrix, provided the precipitate is either non-continuous or has a lower T_c than the matrix. Both of these provisions exist in the material under investigation.

At the highest annealing temperatures, T_c approached that of the as-drawn material, indicating the presence of a very small amount of

precipitate, regardless of annealing time. Annealing at 650°C caused a reduction in T_c to its minimum for the 1 h anneals, a value which was still coincident with those for longer term anneals.

Although the lower T_c indicates a lower solubility limit of Zr in Nb, the fact that it is still invariant with ageing time means that the matrix composition is the same for all these specimens, implying that chemical equilibrium has been achieved in them all. At lower annealing temperatures than 650°C, however, much longer annealing times than 1 h reduced the T_c even further. For example, at 600°C the 1 h anneal produced T_c of 10.67 K, the 24 h anneal a T_c of 10.61 K and the 168 h anneal a T_c of 10.54 K, showing that the matrix was becoming progressively richer in Nb as the annealing time was increased. In this case, T_c is indicative of the volume fraction of precipitate produced during the annealing treatments, the lower the T_c, the more precipitate present.

Implicit in the above, is the fact that the minimum in each isochronal represents the annealing temperature above which chemical equilibrium is achieved, for that particular ageing time. On the decreasing portion of the curves, incomplete precipitation is causing an adjustment in the matrix composition in accordance with the extent of this precipitation. Consequently the T_c here is a measure of the degree of supersaturation of the solid solution, which naturally decreases as the annealing temperature increases. On the increasing portion of the curves, however, the matrix composition depends upon the solubility limit of Zr in Nb, resulting in a T_c which increases with increasing annealing temperature. Consequently all the curves became coincident at annealing temperatures above the minimum in the 1 h isochronal.

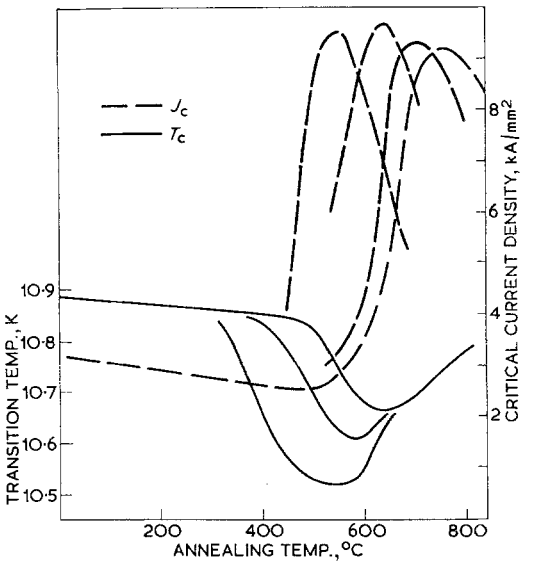

Figure 6 Isochronals of J_c (6.5 K) and T_c versus annealing temperature.

4.2. Metallography

This section can best be followed with the aid of a diagram containing the zero field critical current densities measured by Milne and Ward [17] and the T_c isochronals of figure 1 (see fig. 6). Each set of J_c isochronals divides conveniently into three stages; (*a*) a region where J_c remains relatively unchanged; (*b*) a region where J_c increases rapidly to its maximum value and (*c*) a region where J_c decreases again.

(*a*) This is a region in which both T_c and J_c decrease only slightly. The small change in J_c is common to most studies of this type involving low temperature anneals. Hillmann and Pfeiffer [15] attributed it to dislocation rearrangement. A slight dislocation rearrangement was observed in the present study in specimens annealed for 1 h, resulting in a structure which was less banded than in the as-drawn material. It has been shown [20] that flux pinning is not enhanced by a relatively even dislocation distribution such as this.

(*b*) The minimum in T_c and the steeply increasing portion of the J_c curves typical of this region are accompanied by the structural changes reproduced for the 1 h anneals in figs. 2c to f. The basic linear structure which is increasingly refined as the annealing temperature is increased is accompanied by a varied amount of precipitation.

This highly refined polygonised structure is a feature of all of the peak J_c specimens but the nature of the precipitate has been observed to vary considerably with little effect upon the J_c. For example, annealing below 650°C produced precipitates in amounts which varied with the time at a given annealing temperature, but in a manner which had no consistent correlation with the resultant J_c. Annealing at 650°C, although it has been established that the α_{Zr} was present in the same (equilibrium) quantities regardless of annealing time, produced a critical current density which was still very dependant upon the annealing time. At this temperature the highest J_c was obtained by annealing for 24 h, longer

term anneals causing overageing. A similar behaviour existed at 700 and 750°C, although in the latter case the second phase was identified as β_{Zr}, a superconductive phase with a T_c of approximately 8 K [18]. The quantity of this β_{Zr} present in the samples annealed at 750°C was too small to be observed by dark field electron microscopy.

The equiaxed regions observable in figs. 4b and c and 5a and b are peculiar to the low temperature-long term treatments. Walker, Stickler, and Werner [16] observed similar structures in Nb-Zr after annealing at 700°C for 1 h. From electron diffraction patterns they were claimed to be particles of β_{Zr}, although no dark field microscopy was available to provide positive identification. Subsequent information on the precipitation of β_{Zr} has shown that it occurs in a lamellar or cellular form, growing from heterogeneous nuclei [9, 21, 22] and not as the spherical particles observed above. The relevant dark field microscopy of the present investigation (fig. 5) showed that the equiaxed structures were neither β_{Zr} nor α_{Zr}, but were new crystals of β_{Nb}. This raises additional questions about the recrystallisation temperature of Nb-Zr, being lower than has hitherto been reported [7, 16].

(*c*) This region typifies the overaged condition of the material, the structure of which is totally confused (fig. 4d). Considerable difficulty was encountered in preparing suitable samples for electron microscopy, especially in specimens overaged for longer times, but at lower temperatures however, an equiaxed structure is the dominant feature in all specimens. Despite being overaged, the critical current density of the specimen shown in fig. 4d was usefully high, being about 8.9 kA/mm².

4.3. The Flux Pinning Constituent

Throughout the temperature range, where J_c can be maximised, i.e. 550 to 750°C, several structural features can develop; polygonisation, precipitation of α_{Zr}, precipitation of β_{Zr}, matrix composition changes and the recrystallisation of β_{Nb}. Of these, only the recovered structure can be observed throughout the entire temperature range investigated, although α_{Zr} is also present in varying proportions in specimens annealed up to and including 700°C. Hillmann and Pfeiffer noted that recovery and precipitation were competing processes, and that where precipitation occurred, this became the controlling influence in the J_c characteristics, causing J_c to increase. This competition between recovery and precipitation has not been observed in the present experiment. Indeed it has been shown that the nature of the second phase has no observable influence on J_c in the small quantities precipitated in these specimens. At 750°C for example the precipitating phase, superconductive β_{Zr}, was present in very small quantities yet the J_c obtained was as high as the maximum obtained where α_{Zr} was precipitated. There is as yet no direct evidence of the influence of superconductive precipitates on J_c, although it is generally believed that a superconducting precipitate will not have as large an effect of J_c as a normal one [1, 23].

From the foregoing argument, it seems probable that the structural features most influential in controlling the critical current density of this Nb-25% Zr is the recovered substructure which is developed during the annealing process. This does not mean that precipitates do not influence J_c, but that the small amount of precipitate detected in the present experiments will not do so. In this way, this Nb-Zr must be considered to be similar to the commercially available Nb-44 wt% Ti investigated by Neal *et al* [24]. These authors showed that although the critical current density of their Nb-Ti was enhanced by cold work, additional increases in J_c occurred on annealing to produce the smallest possible polygonised structure with dislocation free cells. Unfortunately, in the present work it was not possible to determine the cell size, since only longitudinal specimens of the wires could be prepared for the electron microscopy.

Other studies on the Nb-44 wt % Ti include that of Baker [25] on the influence of nitrogen doping on the annealing kinetics of this material. He concluded that with interstitials in solution, dislocation mobility is impaired such that ageing temperatures must be raised by 100°C to produce J_c values equivalent to those of non-doped material. This may well account for the lack of consistency in results obtained on Nb-Zr. Here the complications that interstitials influence the monotectoid temperature and the quantity of second phase which precipitates only add to the confusion. It would be interesting to repeat these experiments in full on material which had a higher interstitial content.

5. Conclusions

1. Electron microscopy of Nb-25% Zr wire has shown that, over the range of annealing treat-

ments which maximise J_c, several structural features can develop:
(a) Polygonisation of the dislocation substructure
(b) Precipitation of α_{Zr}
(c) Precipitation of β_{Zr}
(d) Recrystallisation of β_{Nb}.
The change in matrix composition associated with b and c can most easily be followed by T_c measurements.
2. These features do not all occur together, but a is an underlying structure which is developed in all specimens annealed for maximum J_c.
3. A given volume fraction of precipitate can occur in a specimen which has a high or a low J_c.
4. Where superconducting β_{Zr} is present high critical current densities are achieved, so long as 1 a is retained.
5. The combination of 2, 3 and 4 suggest that the flux-pinning constituent in this alloy is the highly refined polygonised dislocation structure and not any of the precipitates.

Acknowledgements

The work was carried out at the Central Electricity Research Laboratories and the paper is published by permission of the Central Electricity Generating Board.

References

1. J. D. LIVINGSTON and H. W. SCHADLER, *Progr. Mater. Sci.* **12** (1964) 183.
2. K. M. OLSEN, R. F. JACK, E. O. FUCHS, and F. S. L. HSU, "Superconductors" AIME conf. 123 (1962).
3. G. D. KNEIP, J. O. BETTERTON, D. S. EASTON, and J. O. SCARBROUGH, *J. Appl. Phys.* **33** (1962) 754.
4. R. G. TREUTING, J. H. WERNICK, and F. S. L. HSU, *Proc. Conf. High Magnetic Fields, MIT* (1962) 597.
5. R. D. CUMMINGS and W. N. LATHAM, *J. Appl. Phys.* **39** (1965) 2971.
6. B. S. CHANDRASEKHAR, M. S. WALKER, H. RIEMERSMA, and F. E. WERNER, *Int. Conf. Low Temperature Physics*, **8** (1962) 345.
7. H. B. SHUKOVSKY, K. M. RALLS, and R. M. ROSE, *Trans. AIME* **233** (1965) 1825.
8. T. KOMATA, K. ISHIHARA, and M. TANAKA, *Jap. J. Metals* **30** (1966) 241.
9. G. W. J. WALDRON, *J. Mater. Sci.* **4** (1969) 290.
10. B. A. ROGERS and D. F. ATKINS, *J. Metals* **7** (1955) 1034.
11. R. F. DOMAGALA and D. J. MCPHERSON, *ibid* **8** (1956) 619.
12. A. C. KNAPTON, *J. Less Common Metals* **2** (1960) 113.
13. C. W. BERGHOUT, *Phys. Letts.* **1** (1962) 292.
14. H. RICHTER, P. WINCIERZ, K. ANDERKO, and U. ZWICKER, *J. Less Common Metals* **4** (1962) 252.
15. H. HILLMANN and I. PFEIFFER, *Z. Metalk.* **58** (1967) 129.
16. M. S. WALKER, R. STICKLER, and F. E. WERNER, *Met. Soc. Conf.* **19** (1962) 4970.
17. I. MILNE and D. A. WARD, "Cryogenics" (1972) (to be published).
18. J. K. HULM and R. D. BLAUGHER, *Phys. Rev.* **123** (1961) 1569.
19. R. F. HEHEMANN and S. T. ZEGLER, *Trans. AIME* **236** (1966) 1594.
20. A. V. NARLIKAR and D. DEW-HUGHES, *J. Mater. Sci.* **1** (1966) 317.
21. G. R. LOVE and M. L. PICKLESIMER, *Trans. AIME* **236** (1966) 430.
22. I. DIETRICH, R. WEYL, and U. ZWICKER, *Z. Metalk.* **53** (1962) 721.
23. J. D. LIVINGSTON, *Appl. Phys. Letts.* **8** (1966) 319.
24. D. F. NEAL, A. C. BARBER, A. WOOLCOCK, and J. A. F. GIDLEY, *Acta Metallurgica* **19** (1971) 143.
25. C. BAKER, *J. Mater. Sci.* **5** (1970) 40.

Received 23 August and accepted 13 October 1971.